Micromechanical Modelling of the Deformation and Damage Behaviour of Al6092/SiC Particle Metal Matrix Composites

Shakir Gatea[1], Tahseen Jwad[2], Fei Chen[3], and Hengan Ou[4]

[1] Department of Materials Engineering, Faculty of Engineering, University of Kufa, Al-Najaf, Iraq

[2] Department of Mechanical Engineering, University of Birmingham, Birmingham, B15 2TT, UK

[3] Department of Plasticity Technology, Shanghai Jiao Tong University, Shanghai, PR China

[4] Department of Mechanical, Materials and Manufacturing Engineering, Faculty of Engineering, University of Nottingham, Nottingham, NG7 2RD, UK

Abstract

To enhance the performance and design of metal matrix composites, it is extremely important to gain a better understanding of how the microstructure influences the deformation and damage behaviour of metal matrix composites under different loading conditions. Finite element (FE) analysis can be used to collect certain micromechanical information of composites that is difficult to obtain from experiments. In this work, the effect of the distance between the SiC particles and the loading conditions on the deformation and damage behaviour of Al6092/SiC particle composites is investigated under different strain rates (i.e., $1x10^{-4}$, $2x10^{-4}$, and $4x10^{-4}$ s^{-1}). A program is developed to generate the 2D micromechanical FE model with 17.5Vol. % SiC particles. Based on the scanning electron microscopy (SEM) images, the FE model contains four SiC particle sizes (3.1, 4.46, 6.37, and 9.98 μm) with various percentages, which are randomly distributed in the micromechanical Al6092 alloy matrix. User-defined field (USDFLD) subroutine was developed and implemented through Abaqus/Standard based on maximum principal stress and Rice-Tracey triaxial damage indicator to evaluate the formability of the aluminium matrix composite (AMC) and to predict the brittle and ductile fracture of the SiC particles and the aluminium matrix, respectively, under tensile and shear loads. The results showed that the distribution of SiC particles in Al matrix has a significant effect on the mechanical properties of Al6092/SiC 17.5 particle composites. The formability and damage behaviour of composites improve as particle distance increases and strain rate decreases under tensile and shear loading. The fracture initiation toughness of fine SiC particles is higher than that of coarse SiC particles.

Keywords: Micromechanical Modelling, Al6092/SiCp composite, Finite element analysis, Damage

Corresponding authors: Shakir Gatea, Shakir.Gatea@uokufa.edu.iq *and* Hengan Ou, H.Ou@nottingham.ac.uk

Nomenclature

USDFLD	User-defined field subroutine
FE	Finite element
SEM	Scanning electron microscopy
AMC	Aluminium matrix composite
σ	True stress
σ_y	Yield stress
σ_m	Hydrostatic stress
σ_{Mises}	Von Mises equivalent stress
σ_f	Failure stress
σ_{max}	Maximum stress
ε	True strain
K	strength coefficient
n	work hardening exponent
η	Stress triaxiality
d	Triaxiality damage indicator
d_{cr}	Critical value of triaxiality damage indicator
$d\varepsilon_p$	Incremental equivalent plastic strain
ε_f	Failure plastic strain
ε_{eq}	Current equivalent strain
ε_f	Failure equivalent strain
f	Exponential failure
m_f	Material constant parameter

1. Introduction

Compared to the monolithic alloys, aluminium matrix composites with SiC particles reinforcement are commonly used in industrial applications such as aerospace and automotive industries due to its superior thermal and mechanical properties. Understanding of the relationship between microstructure, deformation behaviour, initiation of damage, and damage growth in particle metal matrix composites is considered essential for material design and its industrial applications [1]. Finite element (FE) analysis is a powerful tool that could be utilized to model the formability behaviour and damage initiation in particle composite materials under different conditions. Furthermore, it can be used to obtain a micromechanical knowledge of composites in a systematic manner that cannot be obtained from experiments [2].

Over the last few years, several micromechanical FE models have been developed to predict the material's behaviour of particle reinforced metal matrix composites. Elastic-plastic properties of Al/Al_2O_3 particle composite were analysed using the finite element method. The results showed that the mechanical properties of the composite are affected by the grain size of the aluminium matrix [3]. A finite element model of Al6061/20% Al_2O_3particles composite was developed based on viscoplastic behaviour and isotropic strain hardening law to investigate the effect of Al_2O_3 particles on the creeping behaviour of composite material. Reinforcement particles were found to have an effect on creep behaviour and fracture time was shorter for composite material than the Al6061 aluminium alloy matrix [4]. The effect of SiC particle morphology on the mechanical behaver of Al6061/15% SiCp composite was investigated utilizing the FE model with three shapes of SiC particles (circular, angular with sharp corners, and angular with smooth corners). The FE findings indicate that the SiC particle morphology affects the load carried by the particles and that the greatest stress value was correlated with angular SiC particles with sharp corners [2]. A micromechanical FE model was developed to capture the effect of residual stresses on mechanical properties and damage behaviour of Al/10%SiC_p composite under compressive loading. The FE results showed that the effect of residual stresses on damage initiation of Al/SiCp composite is considered low compared to the strain from the externally applied load [5]. Fracture criterion was implemented in the micromechanical FE model to predict the fracture initiation of Al6061/10 vol. % Al_2O_3 particle composite due to the residual thermal stresses. The results demonstrated the ability of the FE microstructural model to determine the effect of residual thermal stress on the damage initiation of particles composite material [6]. The influence of clustered and uniform random arrangement of SiC particles on the damage of Al/SiCp was evaluated utilizing

numerical and probabilistic analysis, however, only brittle fracture of SiCp was considered in this investigation. The investigation found that the probability of damage is increased by the clustered arrangement of the particles [7]. The effect of orientation anisotropy of SiC particles reinforced Al2080 aluminium alloy on tensile properties was evaluated based on modelling and experimental investigation of extruded Al2080/10, 20, 30 vol. % SiCp composites. It was found that higher values of elasticity and tensile strength of composite were exhibited in the extrusion direction as compared to transverse direction [8]. The transition phase of Al/10% SiCp composite was modelled using the FE method to evaluate its effect on the failure of composite material, both ductile and brittle fracture criteria were applied to predict the fracture in the interface region. The results showed that both material properties and dimensions of the transition phase had a substantial effect on the failure of Al/SiCp composite [9]. The relationships between the strength and microstructure of graded Al/SiCp composite was analysed through numerical analysis. It was shown that the degree of gradient of SiC particles has a significant effect on the damage strain, stiffness, and flow stress of Al/SiCp composite. The damage strain is increased with the stiffness and flow stress of composite material decreased by increasing the degree of gradient of SiC particles [10].

The effect of ductile and hard interphases on the strengthening behaviour of the particle metal matrix was investigated numerically. The results of the numerical model pointed out that the hard interphase increases the strength whereas the strength was decreased with ductile interphase of particle composite [11]. Weibull distribution and Eshelby method were employed to develop a mechanical model to predict the tensile ductility and fracture toughness of Al6013/30vol% SiCp composite. The model was found to be ideal for predicting the mechanical response of the Al/SiCp composite, and it was also shown that the tensile strength and fracture strength could be enhanced by the size of the SiC particles [12]. A FE model was developed on the basis of the actual microstructure to test the behaviour of the Al/SiC composite at elevated temperatures. The FE stress-strain results were consistent with experimental results with a small error and the temperature and strain rate have an insignificant effect on the strengthening of Al/SiC composite [13]. The influence of volume fraction, size, random dispersion, and concentration of SiC particle was considered in the FE model to study the indentation behaviour of Al1080/SiC particle composite using spherical indenter. The experimental and FE results showed that higher indentation depth could be achieved with large SiC particles, while the indentation depth was decreased by increasing the volume fraction of particles [14]. Scanning electron microscope images of Al/SiCp composite were transferred to a CAD model subsequently imported into ANSYS to understand the failure

mechanism and predict the strength of composite materials of different microstructures. The findings showed that the clustering of SIC particles in the Al matrix accelerated the fracture of the composite material [15]. The micro stress-strain curve of 6064Al/Sicp composite was investigated using a unit cell model. The cohesive model was considered in order to predict the crack growth of the interface between the aluminium matrix and SiC particles. The stress-strain curve showed that the highest value of stress and deformation occurred in the interface area at a certain angle from the tensile stress direction [16]. Thermo-elastoplastic micromechanics model was built up based on a variational asymptotic method to identify the behaviour of metal matrix composite under thermomechanical loading. The FE model showed that the change in temperature could play an important role in the response of aluminium/boron composite [17]. The effect of boundary conditions (symmetric and periodic), loading type (shear, tensile and combined shear and tensile loads) and interface strength on the mechanical characterization of Al/SiCp composite were investigated using 2D finite element micromechanical model. The results of the micromechanical model showed that the boundary conditions have an insignificant effect on elastic properties of Al/SiCp composite while it plays an important role on the strength properties, also it was found the tensile strength of the interface region could affect the tensile strength of Al/SiCp composite [18, 19]. The mechanical, physical, and fracture toughness behaviour of an A356/0-25wt% SiCp composite was investigated using an ANSYS FE model. The findings were compared with experimental work. It was found that the peak value of tensile strength, flexural strength, and modulus of elasticity of Al/SiCp composite was achieved when the volume fraction of SiCp is 25wt% [20].

From literature, several micromechanical models have been developed to investigate the effect of the microstructure on the mechanical behaviour of the metal matrix composite. The microstructure of the composite material was described using two techniques: in the first method, the digital image techniques with special software are used to transform the actual microstructure (SEM image) to a CAD model and then to build a FE model. Second, the microstructure of composite material is produced automatically using an established program and the FE model can be directly created by this program. Furthermore, it is evident from the literature that the greatest attention has been paid to investigating the effect of the shape and distribution of the particles in the metal matrix, and more work is needed to investigate the effect of different particle sizes in the same micromechanical model, as well as the distance between the SiC particles, on the formability and fracture behaviour of Al6092/SiC particle composites. The objective of this study is to investigate the effect of the

microstructure on the formability and damage behaviour of the Al6092/17.5 percent SiCp composites under tensile and shear loads at different strain rates (i.e., $1x10^{-4}$, $2x10^{-4}$, and $4x10^{-4}$ s^{1}). Four particle sizes, with different percentages, were used in a micromechanical model identical to the actual microstructure. Different distances between the SiC particles were used in order to test the effect of distance on the formability and fracture of the composite. A new code has been created using MATLAB to generate four groups of particle sizes of the composite metal matrix microstructure. These particles were distributed randomly but with predetermined minimum distance between the particles. Maximum principal stress criterion and Rice-Tracey damage indicator were developed utilizing Abaqus/ Standard via user define fields (USDFLD) to assess the formability and predict the damage in SiC particles (brittle fracture) and aluminium matrix (ductile fracture).

2. Material and mechanical properties

In this study, 6092 aluminium reinforced with a 17.5% volume fraction of SiC particle sheet was used to investigate the effect of particle distance and loading conditions on the deformation and damage behaviour of particle composite sheets under different strain rates. Powder metallurgy was used to manufacture the 6092Al/SiC particle composite sheets. Table 1 describes the chemical composition of the aluminium matrix.

Table 1. Chemical composition of 6092 aluminium matrix.

Mg	Si	Cu	Fe	Zn	Ti	O	others	Al
0.8-1.2	0.4-0.8	0.7-1.0	0.3	0.25	0.15	0.05-0.5	0.15	Bal.

To determine the mechanical properties of Al6092-O alloy matrix sheets, a tensile test was performed in accordance with ASTM-E8. The true stress-strain curve of Al6092 alloy can be identified by Ludwik hardening law, as it provided the best fitting of the uniaxial tensile experiment data, as shown in Figure 1. The parameters of the Ludwik Model were as follows: $\sigma_y = 94.5$ MPa, K=165.29 MPa, and n=0.38.

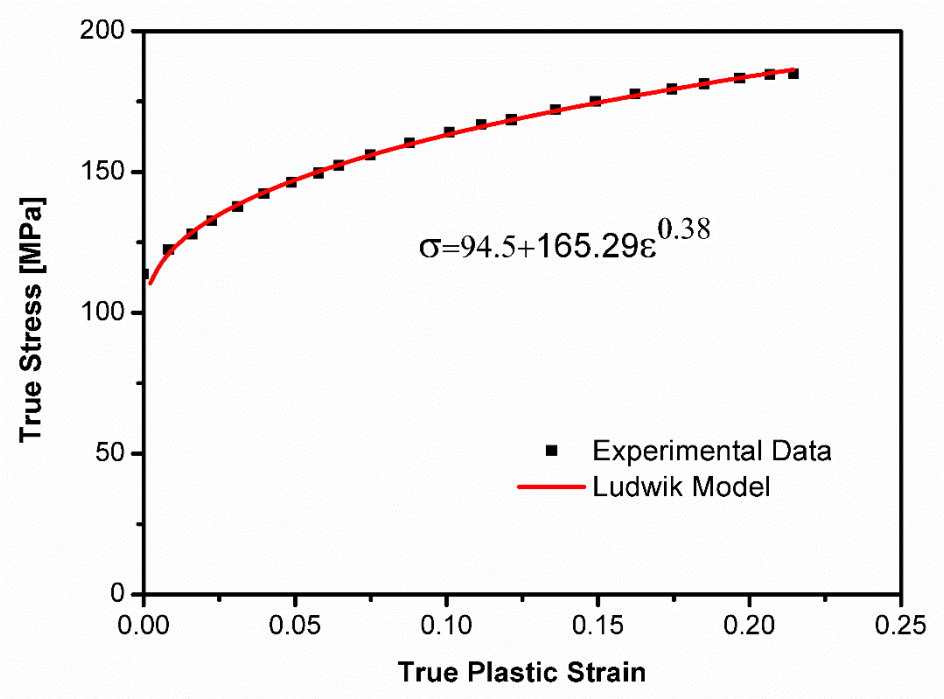

Figure 1. True stress–true plastic strain data of uniaxial tensile test, and the corresponding best fitting curve using Ludwik model.

3. Microstructure design of Al6092/SiC particle composite

A code was written in Matlab to generate four groups of SiC particle size distributed randomly in a field of 100 µm × 100 µm of the 6092 aluminium matrix. The code can be used to calculate the total number of particles, based on their density, of each group of sizes. Then by using the Matlab random number generator function, the (x, y) location (within the field) is located for the bigger particles first. Before finding the (x, y) coordination of the next particle, the code will check the boundary of each particle to be at a minimum distance of a preselected value from other particles or from the edge of the field. After repeating the above for all the groups of particles size, a dxf file will be generated.

4. Finite element model and boundary conditions

The deformation and damage behaviour of Al6092/SiCp composites under tensile and shear loading was investigated using a non-linear FE model (Abaqus/standard). A square two-dimensional (2D) microstructural model of Al6092/SiCp composites was developed with 17.5Vol. % SiC particles. The Al/SiCp composite material was scanned under a scanning electron microscope (SEM), and the SEM images were analysed using ImageJ software to measure the size of the SiC particles, as shown in Figure 2. From the scanning electron

microscopy images, there are four sizes of SiC particles (3.1, 4.46, 6.37, and 9.98 µm) with different percentages as shown in Figure 3. Therefore, in the FE model, there are four particle sizes are scattered randomly in the micromechanical of the Al6092 alloy matrix. The micromechanical model has meshed with 2D 8 node quadrilateral reduced integration element (CPS8R). The developed microstructure's FE model has dimensions of 100 × 100 µm and an element size of 0.4 × 0.4 µm. The total number of elements in the FE model is 66537. The interface between the metal matrix and the ceramic reinforcement is considered important in composite materials, and the properties of the interface region have a significant effect on the mechanical properties of composite materials. Many micromechanical models have been developed to predict fracture growth at the interface and to assess the impact of the interface on the overall properties of composite materials [9, 11, 16, 18, 19]. Some researchers, on the other hand, developed their micromechanical model under the assumption that the bonding between the matrix and reinforcement is perfect [3, 14, 15, 21].

O-condition annealing is used to improve the formability of Al/SiC particle composite sheets and to strengthen the bonding between the hard particle and the metal matrix [1]. Therefore, O-condition annealing was used in this investigation to improve the formability of the composite sheet and the bonding between SiC particles and the Al matrix. As a result, in this study, the bonding was assumed to be perfect in the developed model, and The prediction of the fracture in the Al matrix was given more attention.

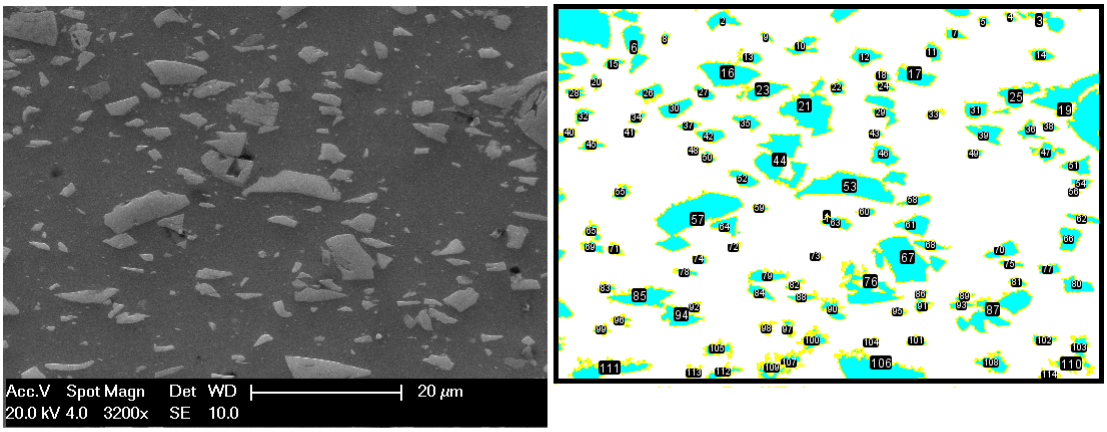

(a) (b)

Figure 2. Determination of SiC particle size using ImageJ software to convert the actual microstracture (a) to the CAD microstracture (b).

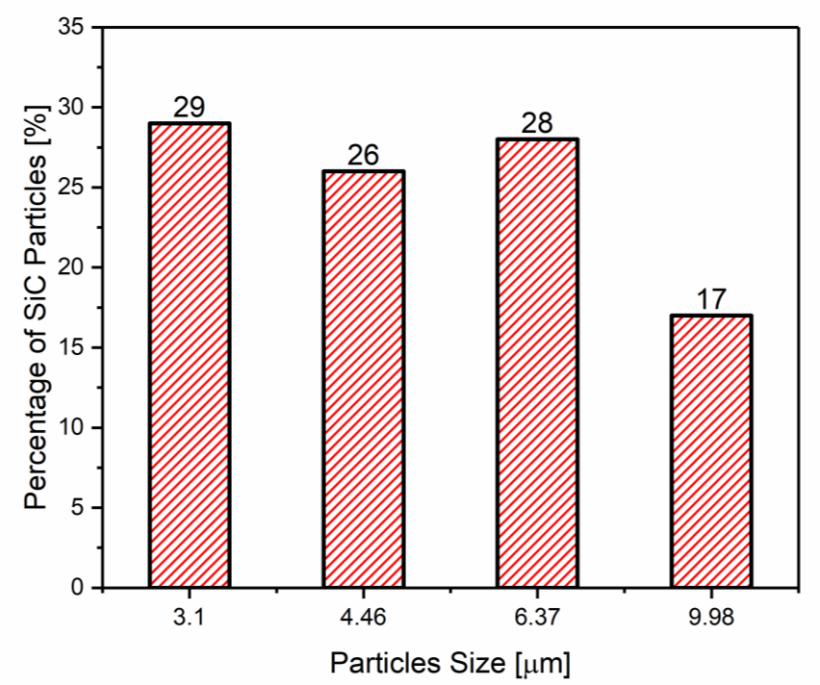

Figure 3. The percentage of SiC particles sizes in Al6092 aluminium matrix.

Six micromechanical models with different distances (minimum distance) between the SiC particles, i.e., 0.25, 0.5, 1, 2, 3, and 4 μm, and each model with different particle sizes (3.1, 4.46, 6.37, and 9.98 μm), were developed to study the influence of the distance between the SiC particles on the formability and damage behaviour of Al composite, as shown in Figure 4. The figure shows that there are many vacancies within the Al matrix without the SiC particles with a small distance between SiC particles (0.25 and 0.5 μm), and uniform distribution of SiC particles can be obtained by increasing the distance between the particles (4 μm). Due to the size of the micromechanical model 100 x 100 μm and the SiC particles percentage, 17.5%, 4 μm is the maximum value of minimum distance between particles that can be used in this investigation.

When the distance between SiC particles decreases for a given volume fraction of SiC particle, two regions in the Al matrix are observed: the first is a high particle density region, and the second is a particle-free region. The formability of high particle density regions is considered low in comparison to particle-free regions because the formability decreases with increasing particle percentage and fracture initiates in these regions [9, 22]. As a result, a uniform distribution of SiC particles in an Al matrix is required to achieve a balance between the composite's formability and strength. The goal of this research is to determine the best particle distance to achieve high formability in Al/SiC particle composites.

In this investigation, aluminium matrix composite sheets Al6092/17.5 Vol. % SiCp with a thickness of 1.04 mm were used. The Al6092/SiCp composite sheet was received at T6 heat-treated condition. The metal matrix composites show poor formability at room temperature due to the brittle reinforcement particles. Therefore, the composite materials always manufacture at elevated temperatures [23, 24]. Besides, the T6 condition works to increase the strength of Al alloys. Therefore, O-condition annealing was carried out in our previous investigation [1], according to the recommendation of ASM [25] to improve the room ductility of Al6092/SiCp composite sheets. Likewise, O-condition annealing was applied to the Al6092 alloy matrix to enhance its mechanical properties and to be comparable with Al6092/SiCp-O composites.

The Al6092-O alloy matrix was modelled as elastic-plastic damageable material, with Poisson's ratio 0.345 and modulus of elasticity 70 MPa. The particles of SiC behaved as isotropic elastic damageable material and its Poisson's ratio 0.14 and modulus of elasticity 410 MPa. The strength of SiC particles follows the distribution of Weibull [19, 26] with an average value of 550 MPa.

In the FE of the developed micromechanical model, the same boundary conditions for real tensile and shear tests were applied. At the bottom edge of both models (tensile and shear model) the $U_x=U_y=UR_z=0$, and at the upper edge of the tensile model a 0.1 tensile strain along Y-axis is applied, while $U_x=UR_z=0$. At the upper edge of the shear model, a 0.1 shear strain along X-axis is applied and $U_y=UR_z=0$. Figure 5 shows the boundary conditions of designed tensile and shear micromechanical models.

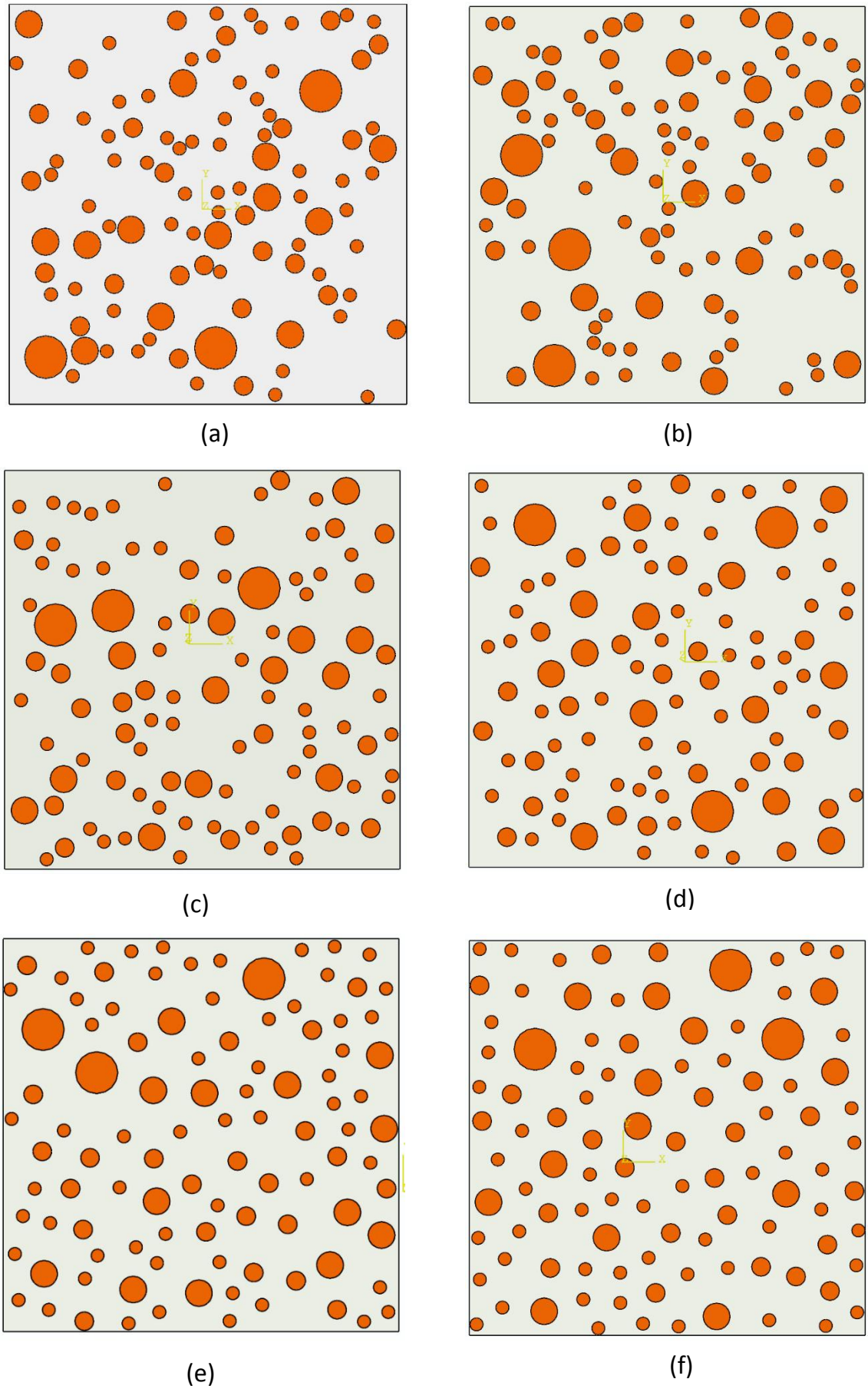

Figure 4. Al/SiCp composite micromechanical models with different distances between SiC particles, (a) 0.25 μm, (b) 0.5 μm, (c) 1 μm, (d) 2 μm, (e) 3 μm, and (f) 4 μm.

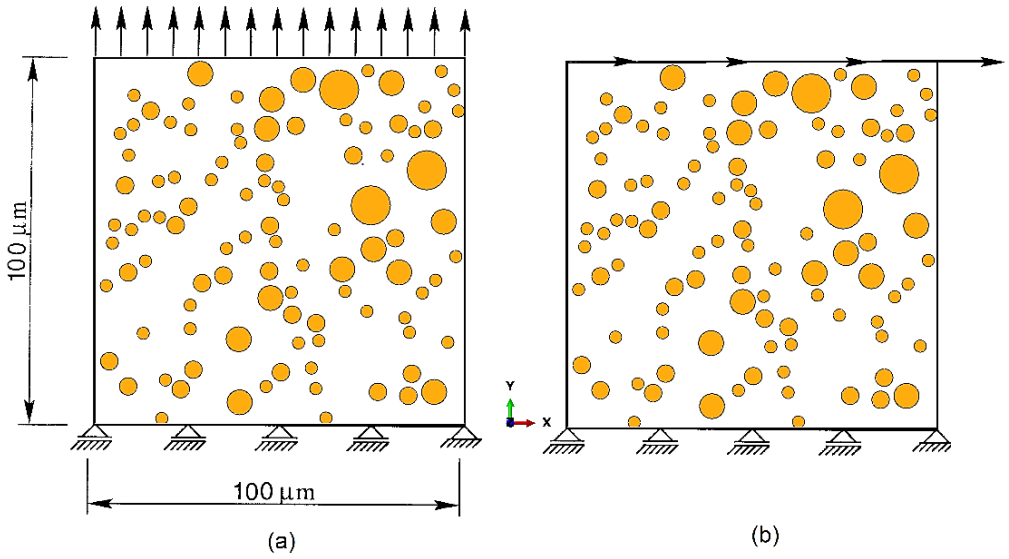

Figure 5. Micromechanical FE model geometry and boundary conditions: (a) tension and (b) simple shear.

5. Damage modelling

The prediction of damage initiation is considered a major challenge. The ductile fracture in metals is developed due to mechanisms such as nucleation, evolution, and coalescence of the micro-voids. In the metal matrix composites, there are three types of failure that can be observed: ductile failure in the matrix material, brittle failure in the ceramic reinforcement, and debonding and fracture at the matrix-reinforcement interface [27].

The stress-strain curve of Al6092 can be characterized by Ludwik elastic-plastic law and is specified as

$$\sigma = \sigma_y + K\varepsilon^n \tag{1}$$

where σ and ε are the true stress and strain respectively, σ_y is the initial yield stress, K is known as the strength coefficient and *n* is the work hardening exponent.

Under external loading, the Al6092 alloy behaves as a ductile material and ductile fracture criterion can be utilized to describe its fracture mechanisms. In this investigation Rice-Tracey [28, 29] triaxiality damage indicator is implemented to predict the damage initiation in the aluminium matrix. The Rice-Tracy function is written in terms of incremental of plastic strain and stress triaxiality ratio as follows:

$$d = \int_0^{\varepsilon_f} e^{1.5\eta}\, d\varepsilon_p = d_{cr} \tag{2}$$

Where d is the triaxiality damage indicator, $d\varepsilon_p$ is the incremental equivalent plastic strain, ε_f is failure plastic strain, η denotes stress triaxiality, $\eta = \sigma_m/\sigma_{Mises}$, σ_m is hydrostatic stress, σ_{Mises} is Von Mises equivalent stress and d_{cr} is the critical value of the triaxiality damage indicator.

The particles of SiC are considered as a brittle isotropic elastic material. The maximum stress failure criterion (Coulomb or Rankine criterion) is normally used to describe the failure in the brittle materials. In this work, this model was implemented to predict the failure of SiC particles. In the maximum stress criterion, the failure occurs when the value of maximum stress ($\sigma_{max.}$) has reached or exceed the value of failure stress (σ_f).

$$|\sigma|_{max.} \geq \sigma_f \tag{3}$$

To describe the post-failure in the brittle particles (SiC particles), the exponential failure equation [19] was employed. Exponential failure (f) is a function of current equivalent strain (ε_{eq}), failure equivalent strain (ε_f), and material constant parameter (m_f) and is specified as:

$$f = \min\left(1, \frac{1 - e^{\left(-m_f \frac{\varepsilon_{eq} - \varepsilon_f}{\varepsilon_f}\right)}}{1 - e^{(-m_f)}}\right) \tag{4}$$

FE approach was used to simulate the damage initiation, evolution, and crack in both the aluminium matrix and SiC particles reinforcement utilizing the approach of element weakening. The user defined field (USEDFLD) subroutine was developed and implemented in Abaqus/Standard to realize the ductile and brittle failure mechanisms of aluminium matrix and SiC particle reinforcement, respectively. In the user Subroutine, the phase of the composite material is defined via the field variable. Based on the field variable, the USDFLD calculates either ductile damage (Rice-Tracey criterion) in the aluminium matrix or brittle failure (maximum principal stress) in SiC particles. If the value of the ductile damage parameter (d) exceeds the corresponding critical value (d_c) of aluminium alloy matrix or the exponential failure (f) of SiC particle is equal to 1, the stiffness of the element is reduced, and the modulus of elasticity is set a lower value about 0.01% of the initial value.

The critical value of the triaxiality damage parameter of Al6092 alloy was determined using a tensile test. The value of d_c was changed in the FE model (0.05, 0.1, 0.15, 0.2, 0.3, 0.4, and 0.45) of a single element to get the best correlation with the experimental curve of stress-strain. The comparison between the experimental curve of the stress-strain and FE model with different values of d_c is shown in Figure 5. It is clear from the figure there is a good correlation between the FE model and the experimental curve when the d_c value is 0.4. Therefore, the

triaxiality damage parameter with a value of 0.4 was used in this study to predict the damage initiation in the Al6092 aluminium alloy matrix. Figure 7 depicts the tensile fracture surface morphology of O-condition annealed Al/SiCp composite sheets. It is observed that the fracture surface has a limited number of SiC particles with a high percentage of dimples. This is because the forming ability of composite sheets is enhanced under O-condition, and the Al matrix is elongated to cover the SiC particles.

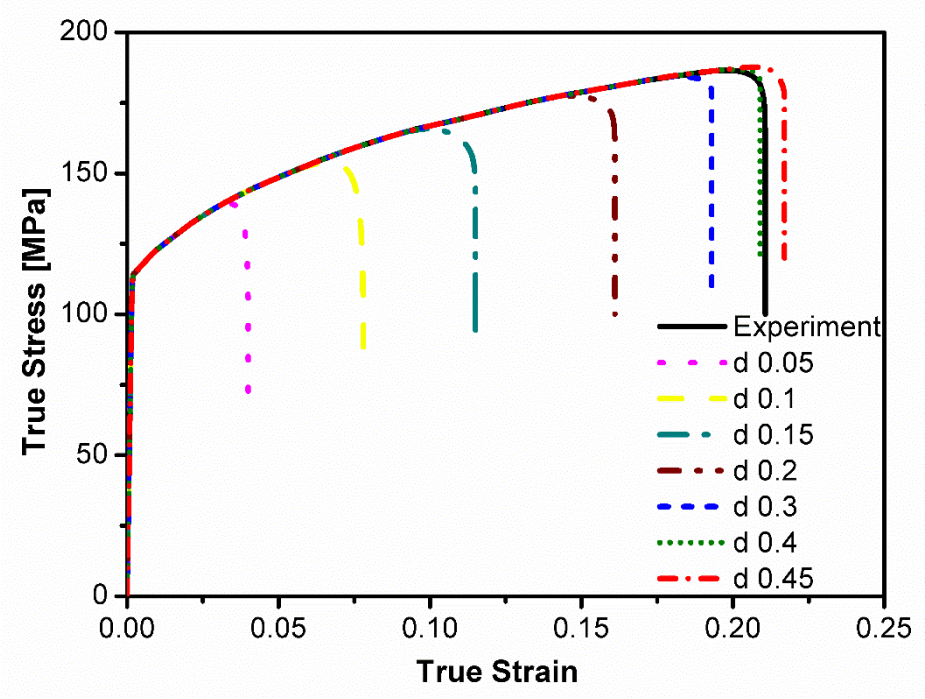

Figure 6. Stress-strain curves of Al6092 alloy with different values of damage parameter in comparison with experimental data.

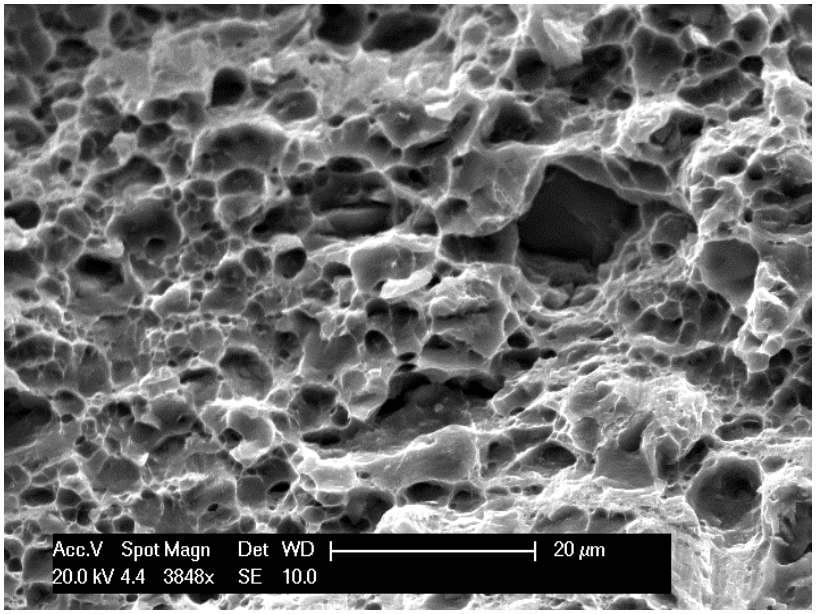

Figure 7. Tensile fracture surface of annealed Al/SiCp composite sheets.

6. Results and discussion

6.1. Influence of particle size

The SEM images of the Al/SiCp composite show four sizes of SiC particles distributed in the aluminium matrix, approximately 3.1, 4.46, 6.37, and 9.98 μm. The maximum value of equivalent plastic stress and damage indicator were evaluated from various particle sizes and under different loading conditions (tensile and shear loading) to investigate the impact of particle size on the formability and damage of Al/SiCp composite. Figure 8 depicts the equivalent plastic stress around varying sizes of SiC particles in the same model with a spacing between SiC particles of 0.25 μm. The figure shows that the equivalent stress around the particles increases with particle size, with higher stress induced around large particles under different loading conditions (tensile and shear load). Figure 7 depicts the damage parameter indicator (Rice-Tracey triaxial damage) around different sizes of SiC particles in the same model under tensile and shear load. The damage accumulation is accelerated around the large particle, as seen in the figure, and tensile loading has a greater impact on the damage values than shear loading. Figure 9 (a) shows that the damage occurs earlier, around the big particles, at 9.98 μm (see Figure 10). The high stress concentration and strain hardening around the SiC particles as well as the large contact area between the SiC particles and the Al matrix can be attributed to the easy fracture around the large size of SiC particles.

According to the equivalent stress and damage parameter distributions under tensile and shear loading, high formability can be accomplished around small particle sizes, whereas fracturing occurs earlier under tensile loading around large particle sizes. The overall nominal stress values (entire stress of composite model) with a spacing between SiC particles of 0.25 μm were determined within the SiC particles and are shown in Table 2. According to the table, as particle size decreases, the maximum value of nominal stress changes and the minimum value of nominal stress is generated within the small SiC particle under tensile and shear loading. Under tensile and shear loading conditions, the maximum nominal stress within the Al/SiC particles increases by 24% and 45%, respectively, when the particle size is changed from 3.1 to 9.98 μm.

Table 2. Maximum nominal stress in SiC particles under tensile and shear load.

Particle size (μm)	Nominal tensile stress (MPa)	Nominal shear stress (MPa)
3.1	156.819	59.881
4.46	165.633	67.103
6.37	178.027	82.119
9.98	194.635	86.908

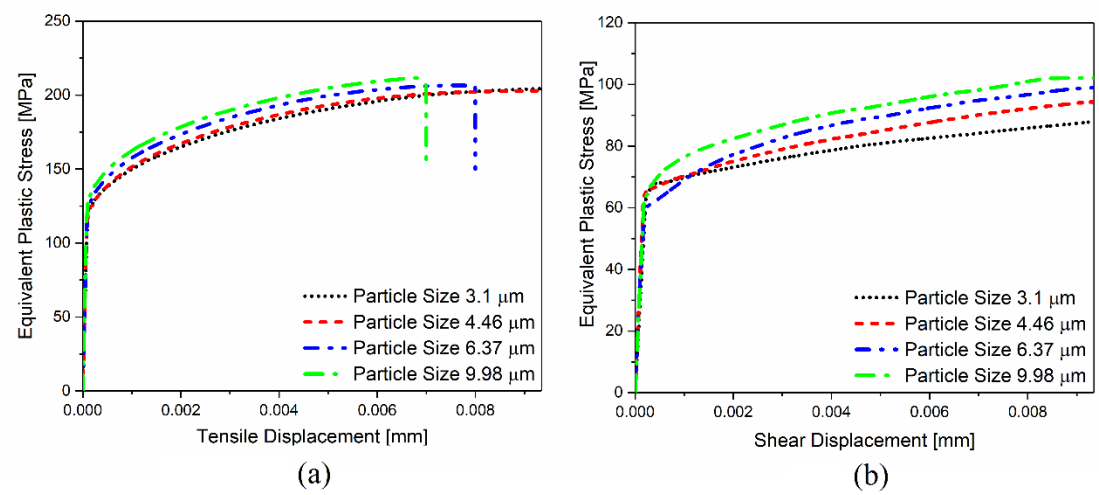

Figure 8. Equivalent plastic stress around SiC particles under tensile condition (a) and shear condition (b).

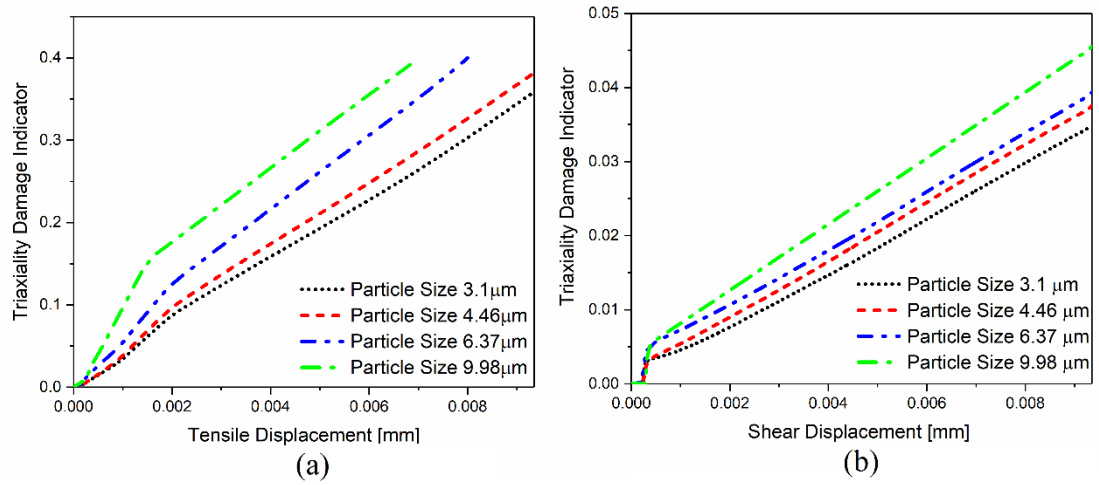

Figure 9. Triaxiality damage indicator around SiC particles under tensile (a) and shear (b) conditions.

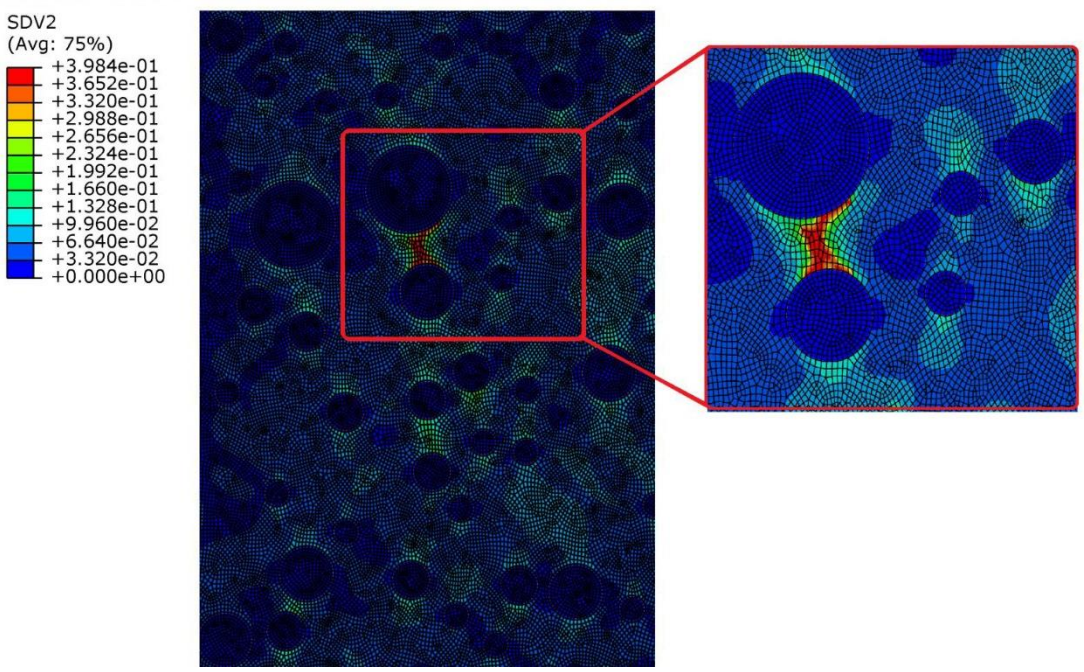

Figure 10. Simulated results of damage around SiC particle from Rice-Tracey triaxial damage model.

6.2. Influence of particle distance and strain rate under tensile loading

To investigate the influence of particle distance and strain rate on the formability and damage behaviour of Al/SiCp composites, a micromechanical model of pure tensile and shear loads was performed under various distances between SiC particles (0.25, 0.5, 1, 2, 3, and 4 µm) and strain rates ($1x10^{-4}$, $2x10^{-4}$, and $4x10^{-4}$ s^{-1}). Both tensile and shear models were subjected to a 0.1 strain in the plane stress condition during the study. Figure 11 depicts the influence of SiC particle distance on the overall tensile nominal stress-strain curves at various strain rates. It is clear from the figure that when the distance between particles is small (0.25, 0.5, and 1 µm), the fracture of the composite material is accelerated, and the formability is improved when the distance between particles is increased (2, 3, and 4 µm) with all strain rates. For a distance of 0.25 µm between SiC particles, the nominal fracture strain is decreased by 17 percent as the strain rate varies from $1x10^{-4}$ to $4x10^{-4}$ s^{-1}, and this percentage is reduced to 7 when the distance between particles increases (e.g., 0.5 and 1 µm). Although no cracking occurs with large displacement (2, 3, and 4 µm), this indicates that composite materials with small distances between particles are more sensitive to strain rate than large distance, and the formability is enhanced when the distance between particles becomes large and uniform. The distance between particles has a greater influence on the nominal fracture strain than the strain rate. As the distance increased from 0.25 to 1 µm, the fracture strain increased by 50%,

53%, and 68%, with strain rates of $1x10^{-4}$, $2x10^{-4}$, and $4x10^{-4}$ s^{-1}, respectively. Under all strain rates, no fracture occurs with large displacement (2, 3, and 4 µm) as shown in Figure 12.

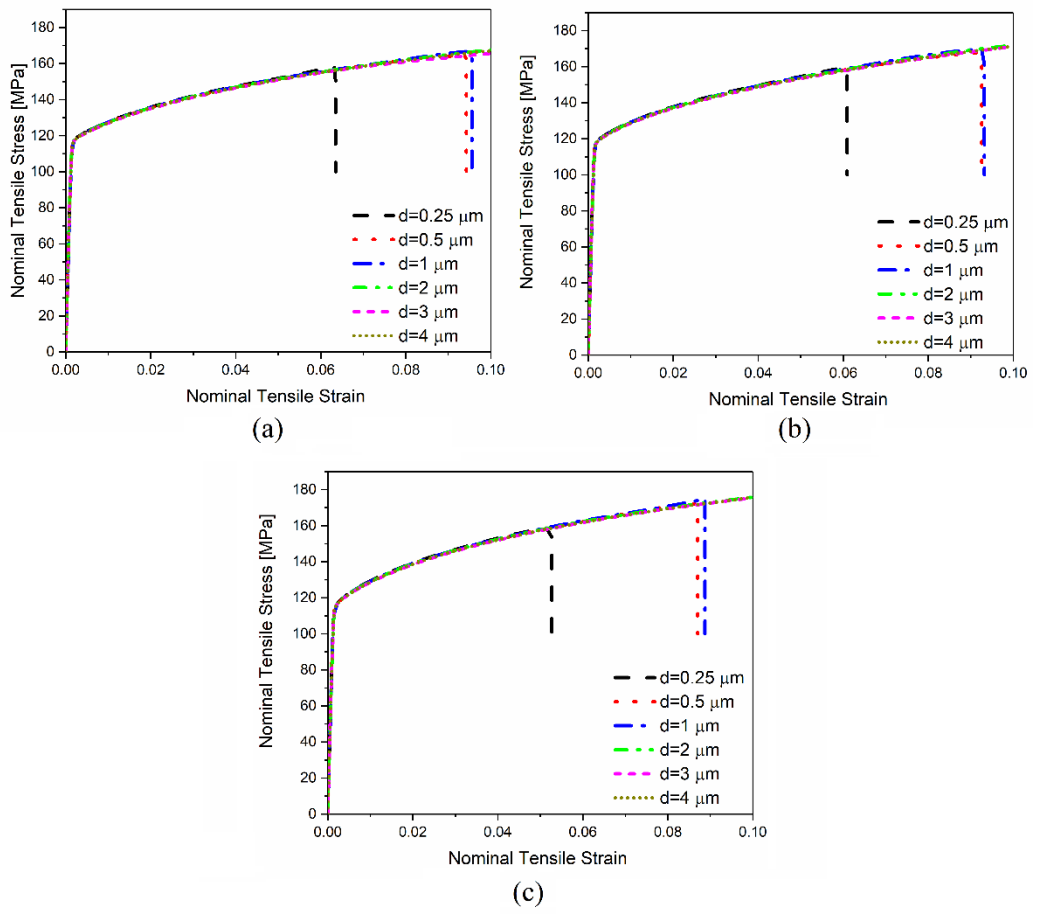

Figure 11. Overall uniaxial tensile nominal stress–strain curves of composites at various SIC particle distances, (a) strain rate $1x10^{-4}$ s^{-1}, (b) strain rate $2x10^{-4}$ s^{-1}, and (c) strain rate $4x10^{-4}$ s^{-1}.

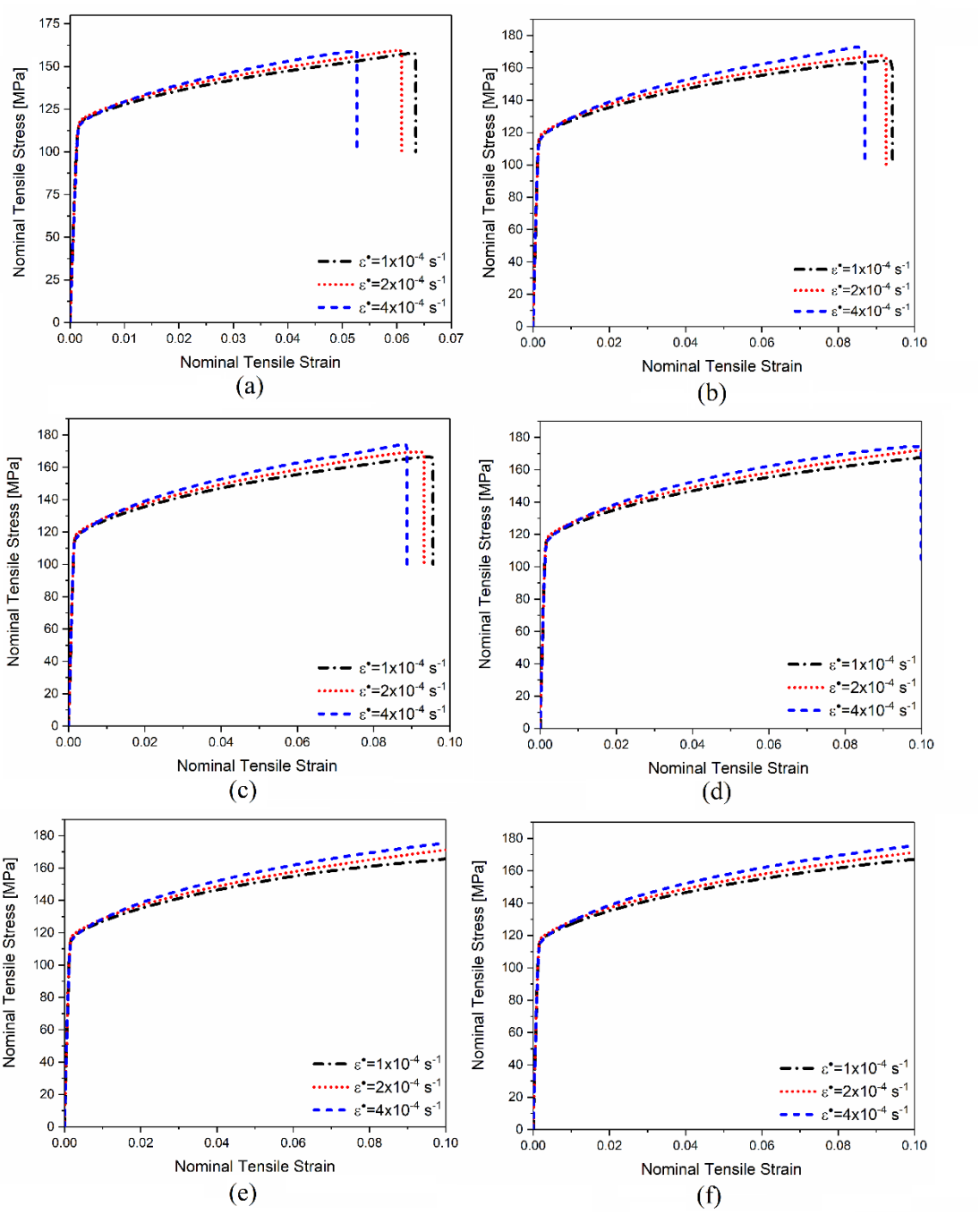

Figure 12. Overall uniaxial tensile nominal stress–strain curves of composites under different strain rates, (a) distance between particles 0.25 µm, (b) distance between particles 0.5 µm, (c) distance between particles 1 µm, (d) distance between particles 2 µm, (e) distance between particles 3 µm, and (f) distance between particles 4 µm

Figure 13 depicts the predicted growth of damage under tensile load in the Al matrix using the Rice-Tracey triaxial damage indicator at various distances and strain rates. The figure clearly shows that under constant strain rate, the small distance between particles causes the damage to grow faster, and larger distance causes the damage to grow slower. The strain rate has a significant effect on the growth of the damage; the cumulative damage increases with the strain rate and fracture occurs earlier in composites when the strain rate is high. For small distance models (0.25, 0.5, and 1 μm), the accumulated value of the damage reaches the critical value (0.4) under all strain rates, while the tensile test of composite is performed without fracture as the distance is increased (2, 3, and 4 μm). Both distance between SiC particles and strain rate have a direct impact on the formability and damage growth of composite materials, but the distance between particles is considered to be more significant than strain rate. The micromechanical tensile model fails before reaching the applied strain (0.1) at all strain rates when the distance between particles is small (0.25, 0.5, and 1 μm), but it performs without failure when the distance between particles is high (2, 3, and 4 μm). However, as the strain rate varies from $1x10^{-4}$ to $4x10^{-4}$ s^{-1} in the model of 2 μm distance between particles, the damage value increases by 29 %, and this amount decreases to 14 % as the distance between particles increases to 4 μm. As the distance between particles is changed from 0.25 to 4 μm, the maximum value of damage decreases by 51 % under a constant strain rate ($1x10^{-4}$ s^{-1}) and by 43 percent under a $4x10^{-4}$ s^{-1} strain rate (see Figure 14).

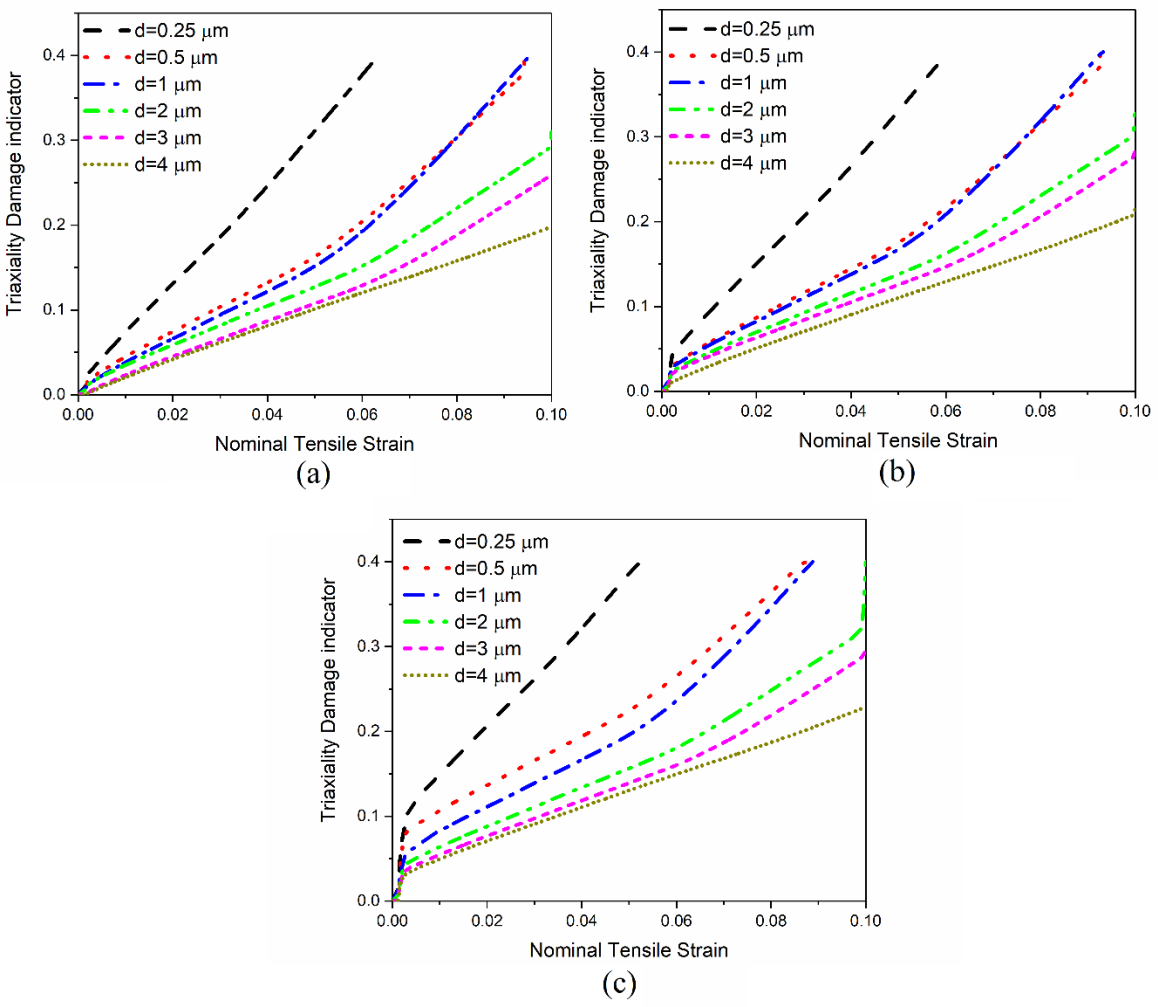

Figure 13. Triaxiality damage indicator of composites at various SIC particle distances under tensile loading, (a) strain rate $1x10^{-4}$ s^{-1}, (b) strain rate $2x10^{-4}$ s^{-1}, and (c) strain rate $4x10^{-4}$ s^{-1}

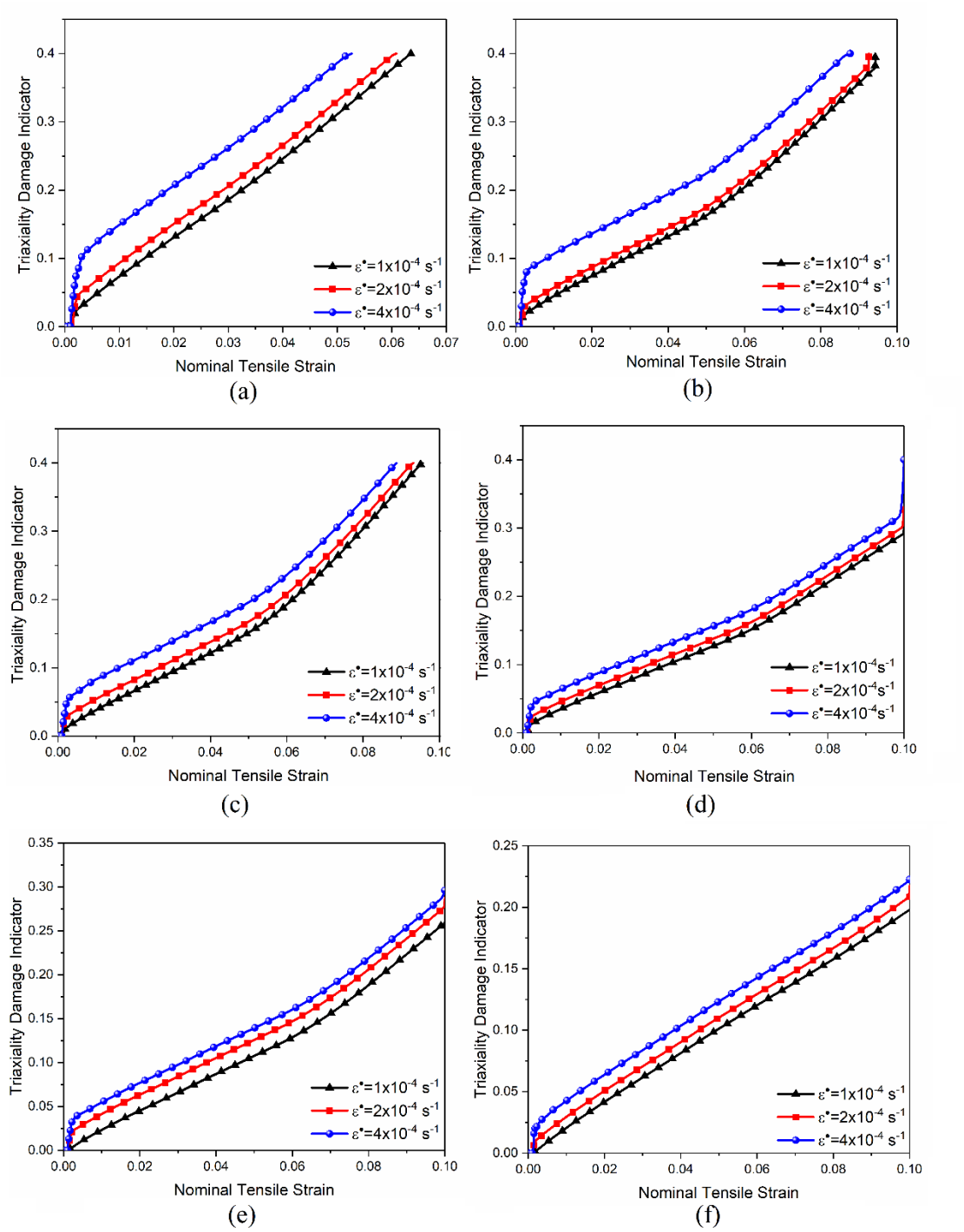

Figure 14. Triaxiality damage indicator of tensile test under different strain rates, (a) distance between particles 0.25 µm, (b) distance between particles 0. 5 µm, (c) distance between particles 1 µm, (d) distance between particles 2 µm, (e) distance between particles 3 µm, and (f) distance between particles 4 µm

6.3. Influence of particle distance and strain rate under shear loading

Under the same conditions as the tensile test, the effect of strain rate and distance between SiC particles on the formability and damage behaviour of Al/SiCp composites under shear load was investigated. Figure 15 depicts the effect of strain rate and particle distances on the overall nominal shear stress. The figure shows that all of the models reach the applied shear strain (0.1) without fracture; additionally, The spacing between SiC particles has little influence on the nominal stress, whereas strain rate affects the values of the overall nominal shear stress, as shown in Figure 16. Under all distances between SiC particles, the maximum value of overall nominal shear stress increases by 4% when the strain rate changes from $1x10^{-4}$ to $4x10^{-4}$ s^{-1}.

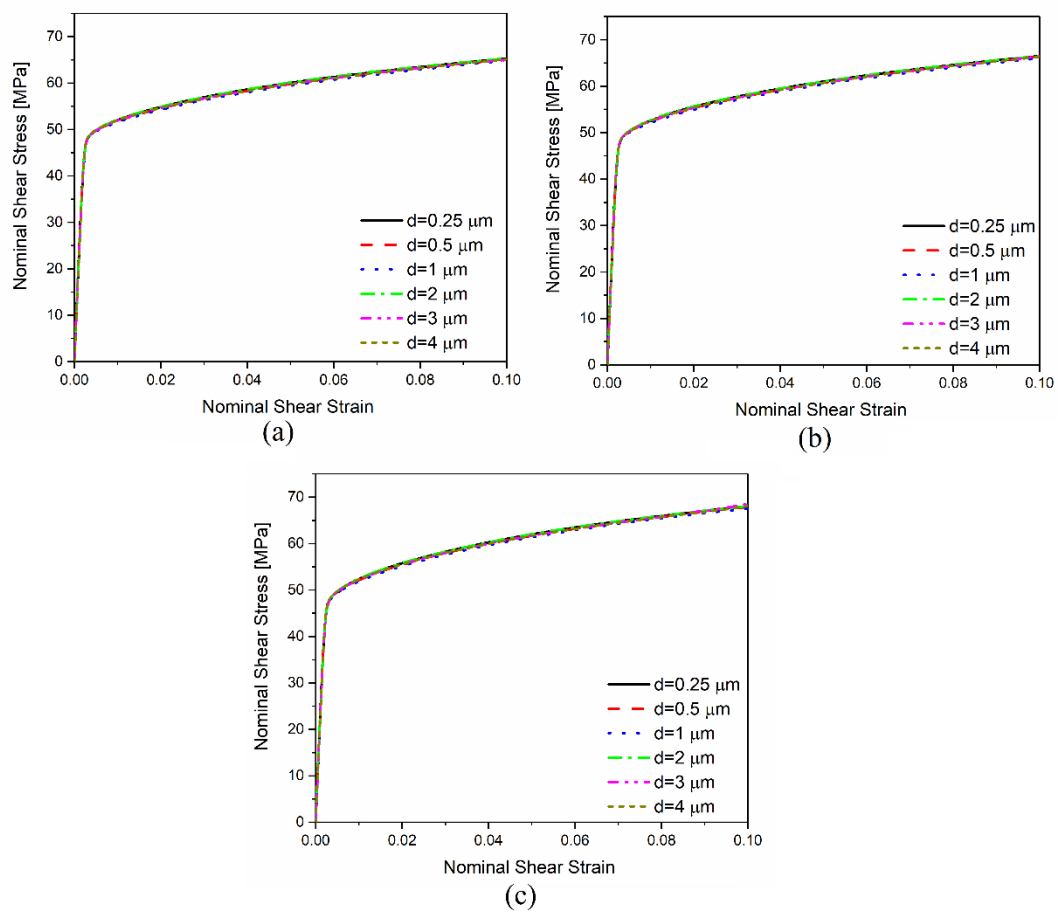

Figure 15. Overall nominal shear stress–strain curves of composites at various SIC particle distances, (a) strain rate $1x10^{-4}$ s^{-1}, (b) strain rate $2x10^{-4}$ s^{-1}, and (c) strain rate $4x10^{-4}$ s^{-1}.

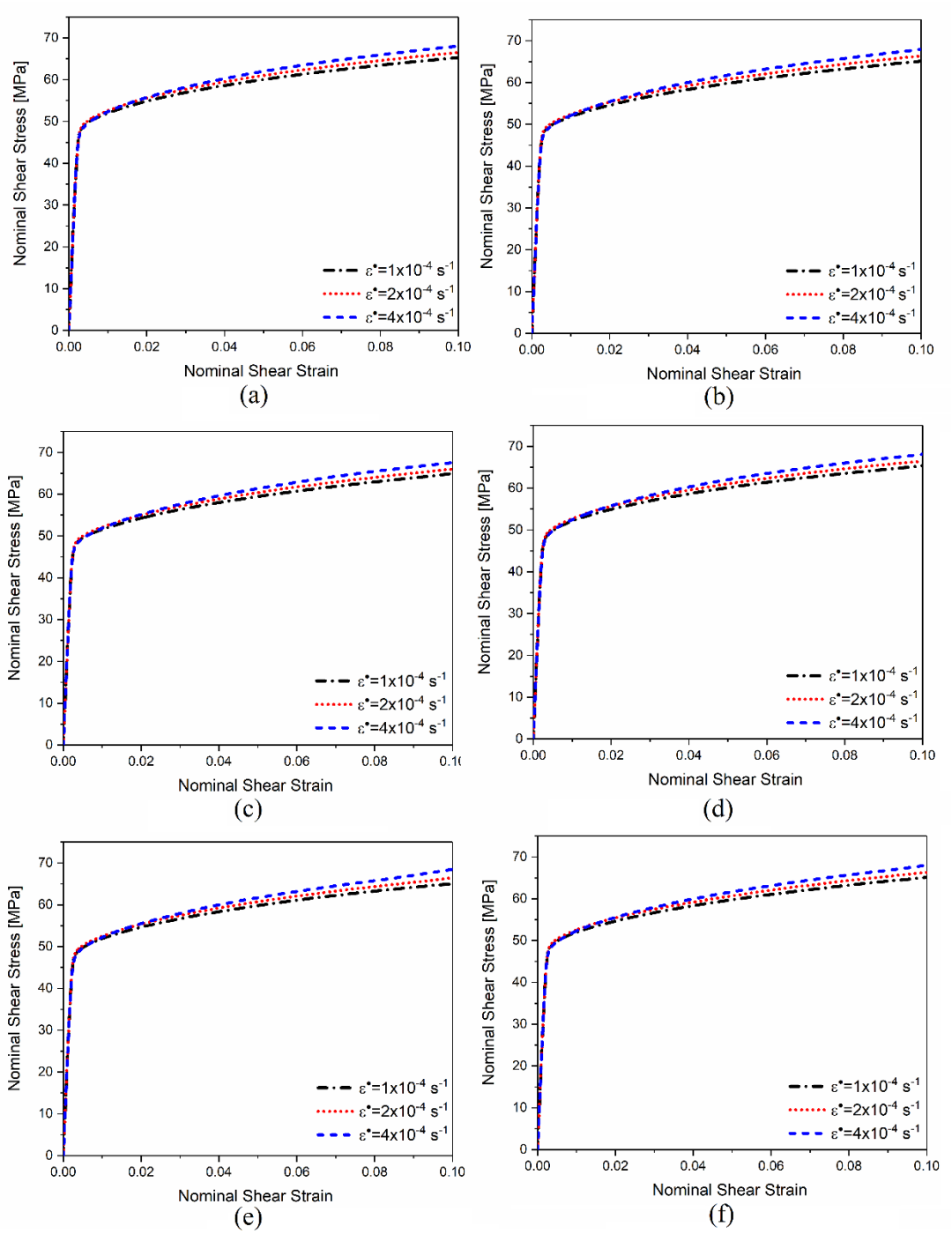

Figure 16. Overall nominal shear stress–strain curves of composites under different strain rates, (a) distance between particles 0.25 µm, (b) distance between particles 0.5 µm, (c) distance between particles 1 µm, (d) distance between particles 2 µm, (e) distance between particles 3 µm, and (f) distance between particles 4 µm

Figure 17 illustrates the effect of strain rate on the damage behaviour of Al/Sic particle composites under shear load with varying distances between SiC particles. The figure clearly shows that both strain rate and particle distance have an effect on the formability and fracture of Al/SiCp composites under shear loading. The damage indicator values decrease as the distance between particles increases and the strain rate value decreases. This means that under shear loading, the formability of Al/SiCp composites is improved by a low strain rate and a large distance between particles. Under shear loading, the damage indicator values are small in comparison to the Al matrix's critical value of damage (d=0.4) under all conditions. This means that the shear test is completed without fracture at the applied shear strain (0.1). When the distance between particles is 0.25 µm, the triaxiality damage indicator increases by 10% when the strain rate changes from 1×10^{-4} to 4×10^{-4} s^{-1}, and this percentage decreases to 5.4% when the distance between particles is 4 µm. Under a constant strain rate (1×10^{-4} s^{-1}) the damage value decreases by 38% when the distance between particles changes from 0.25 to 4 µm, and this percentage increases to 40% under a strain rate of 4×10^{-4} s^{-1} (see Figure 18).

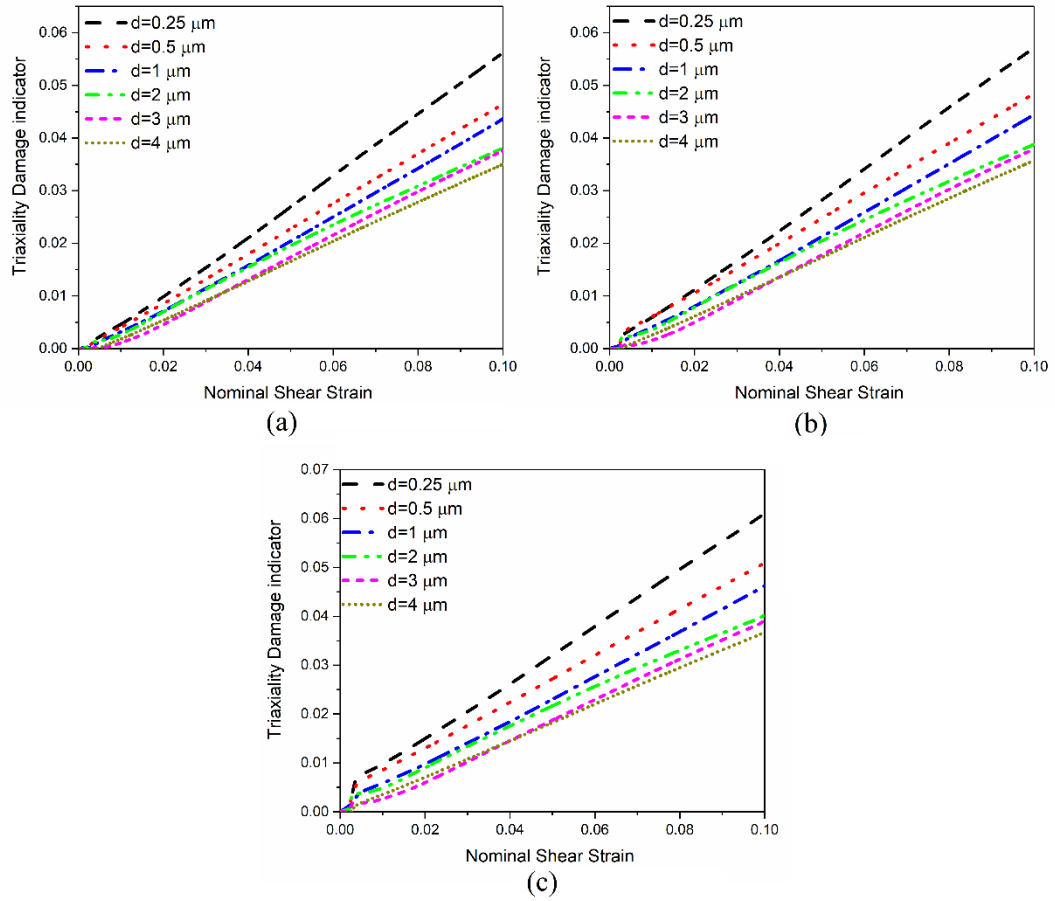

Figure 17. Triaxiality damage indicator of composites at various SiC particle distances under shear loading, (a) strain rate $1x10^{-4}$ s^{-1}, (b) strain rate $2x10^{-4}$ s^{-1}, and (c) strain rate $4x10^{-4}$ s^{-1}

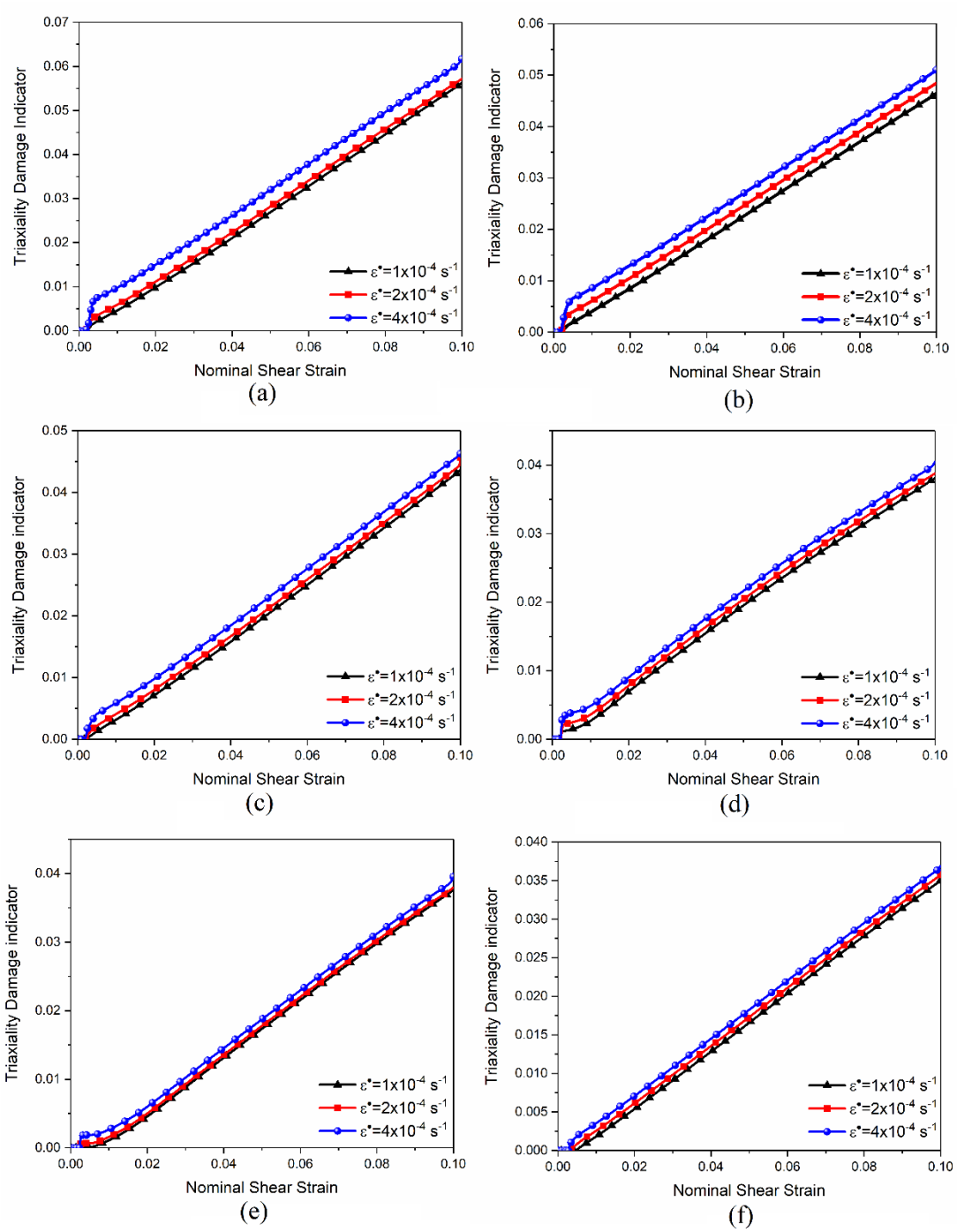

Figure 18. Triaxiality damage indicator of shear test under different strain rates, (a) distance between particles 0.25 µm, (b) distance between particles 0. 5 µm, (c) distance between particles 1 µm, (d) distance between particles 2 µm, (e) distance between particles 3 µm, and (f) distance between particles 4 µm

It can be concluded that decreasing the spacing between SiC particles results in vacancies in the Al matrix without SiC particles, and SiC particles are concentrated in some regions, resulting in weak regions between particles that contribute to reduced formability and accelerate damage initiation under tensile and shear loading. The Al/SiC particle composite's strength rises with strain rate, and the greatest strength is achieved with 4×10^{-4} s^{-1} under tensile and shear loading.

Figure 19 depicts the influence of strain rate and spacing between SiC particles on the highest values of the damage indicator of an Al/SiC particle composite under tensile and shear loading. It is evident from the figure that the tensile test has a greater influence on the damage behaviour of the Al/SiCp composite than the shear test. The greatest value of damage triaxiality reaches the critical value (0.4) in tensile tests with small distances between particle models (0.25, 0.5, and 1 µm) for all strain rates, whereas in shear tests with 0.25 µm distance between particles and $1x10^{-4}S^{-1}$ strain rate, the value of the damage is 0.062. When the distance between particles under tensile loading increases from 0.25 µm to 4 µm under strain rates of $1x10^{-4}$ s^{-1}, $2x10^{-4}$ s^{-1}, and $4x10^{-4}$ s^{-1}, the maximum values of the damage triaxiality indicator decrease by 51%, 46%, and 43%, respectively, whereas this reduction is decreased to 37.7%, 37.5%, and 40% under shear loading.

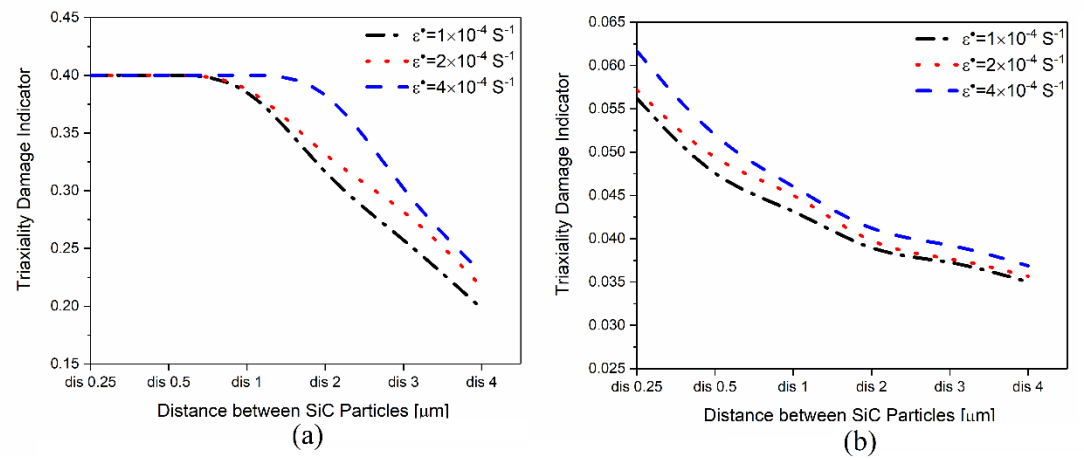

Figure 19. Predicated values of maximum triaxiality damage indicator under different strain rates and distances between particles under (a) tensile loading, and (b) shear loading.

6.4. Validation of designed microstructure model

The actual microstructure of an Al6092/SiC particle composite obtained by scanning electron microscopy is converted to a CAD model, as illustrated in Figure 20. The CAD model is imported into Abaqus/ Standard to validate the designed microstructure (MATLAB model) of

varied SiC particle sizes. The FE models of designed and actual microstructure have dimensions of 47.5 × 31 µm, with an element size of 0.1× 0.1 µm. To validate the designed model with varied particle sizes, the same boundary conditions as in Figure 5 were applied to the real and designed models. The total number of elements for each model (designed and real microstructures) is 147250 elements. Under tensile and shear loading at varied strain rates, the overall stress-strain curves and triaxiality damage indicator of the designed Al/SiC particle composite microstructure were compared to the real microstructure. Figure 21 depicts the overall stress-strain curves of both the designed and real microstructures at different strain rates. The figure clearly shows that when the strain rate changes from 1×10^{-4} s^{-1} to 4×10^{-4} s^{-1}, tensile stress increases and tensile strain drops for both microstructures which is consistent with previous research by Gatea et al. [1]. The simulated tensile stress-strain curves of the designed microstructure correlate with one of the real microstructures. Figure 22 demonstrates the triaxiality damage indicator for both microstructures under tensile loading. According to the figure, damage accumulation accelerates with strain rate, and failure occurs earlier with a higher strain rate. It is also evident from the figure that there is a strong link between the damage of the designed and real microstructure with small error due to the shape of the SiC particles.

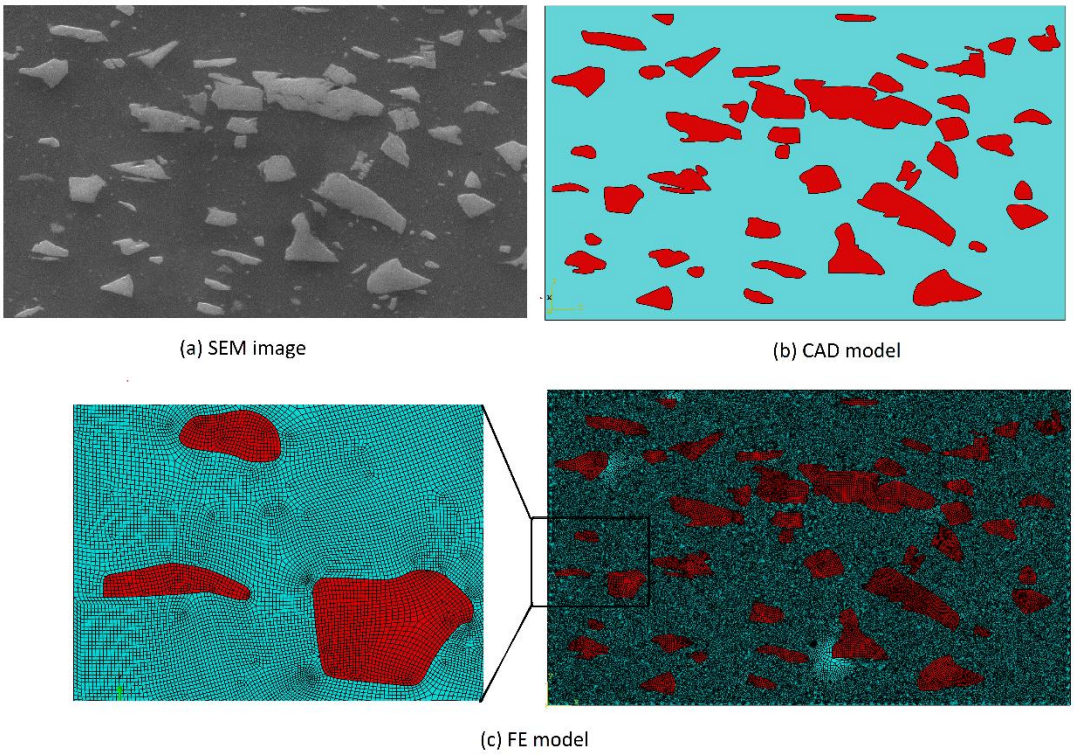

Figure 20. Stages of conversion of real microstructure of Al/Sic particle composite into FEA model.

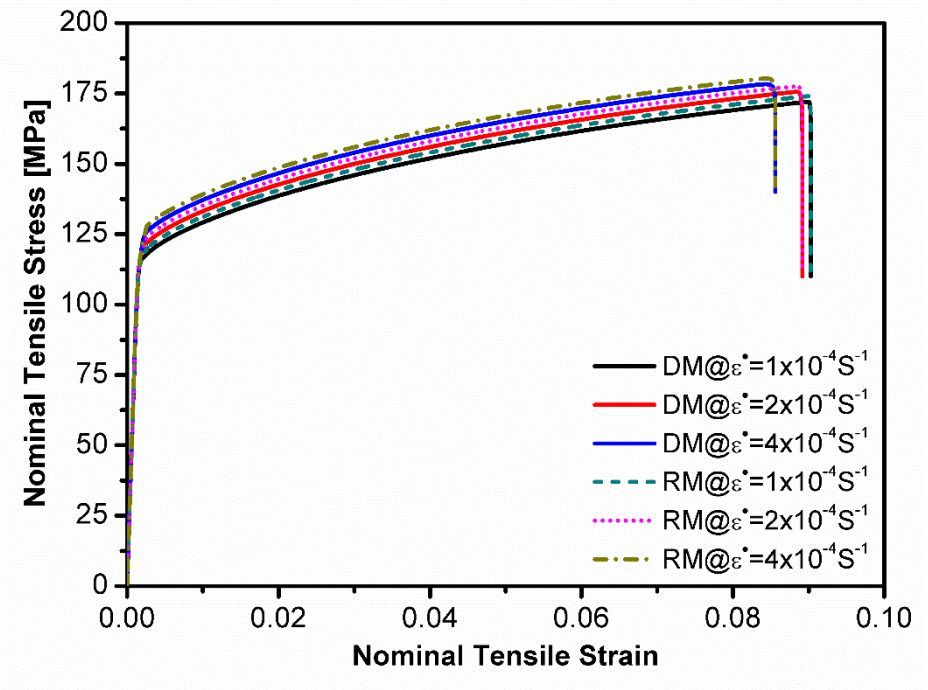

Figure 21. Comparison of overall tensile stress-strain curves of the designed (DM) and real (RM) microstructures at different strain rates.

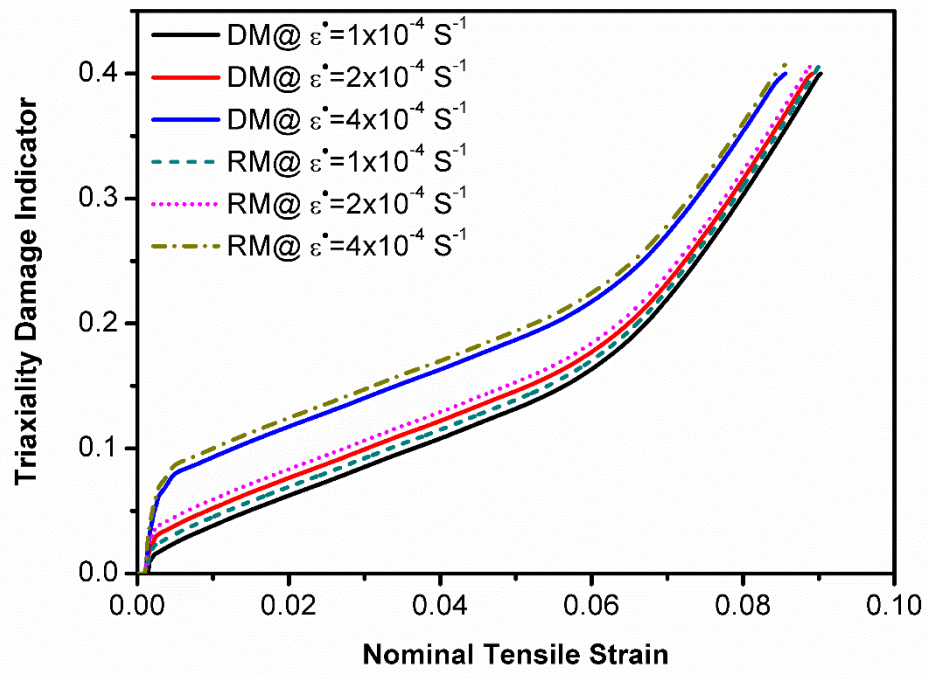

Figure 22. Comparison of the damage indicator of the designed microstructure (DM) and the real microstructure (RM) due to tensile stress at various strain rates.

Figures 23 and 24 demonstrate the influence of shear loading on the formability and damage behaviour of designed and real microstructures of Al/SiC particle composites at different strain rates. It is evident from the figures that the highest values of shear stress and damage indicator are considered minor when compared to the tensile loading, and a similar pattern to the tensile loading is seen, the overall shear stress and the damage indicator rise as the strain rates increase. The designed and real microstructures under shear loading with varied strain rates show a good correlation in the overall shear stress-strain curves and triaxiality damage indicator with a degree of difference due to the shape of the SiC particles.

It can be concluded that the designed microstructure of Al/SiC particle composite may be utilized to predict the formability and damage behaviour of the composite under varied loading (tensile and shear loading) and strain rates, as shown in Figures 21 to24.

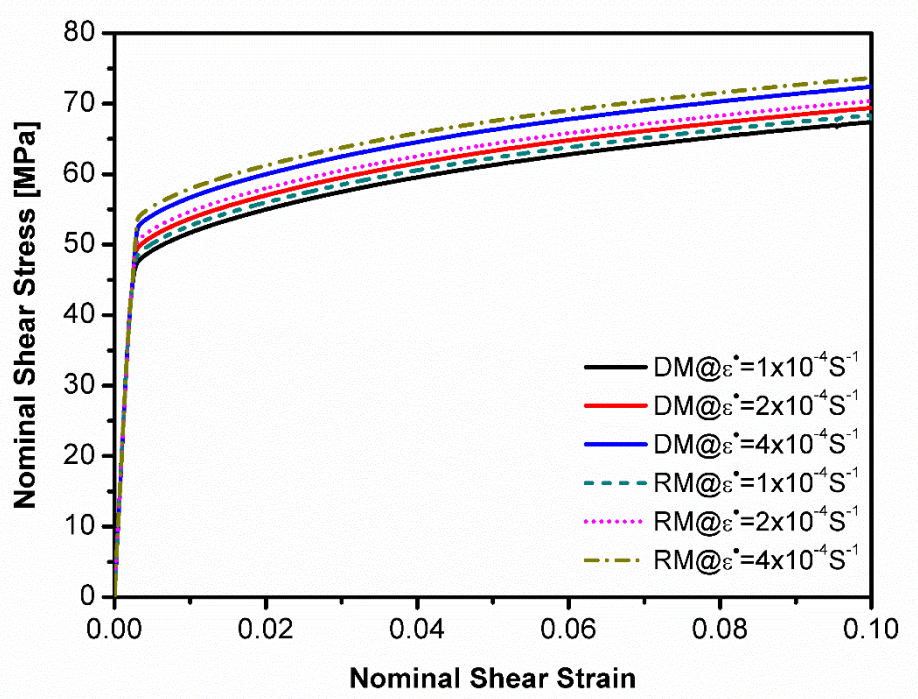

Figure 23. Comparison of overall shear stress-strain curves of the designed (DM) and real (RM) microstructures at different strain rates.

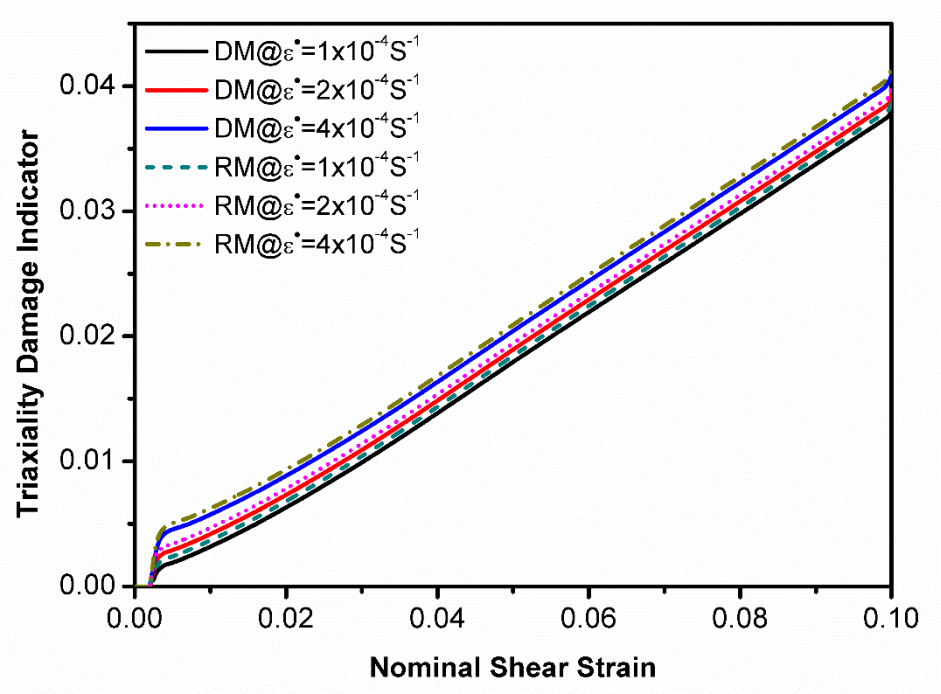

Figure 24. Comparison of the damage indicator of the designed microstructure (DM) and the real microstructure (RM) due to shear stress at various strain rates.

7. Conclusions

Understanding the relationship between the microstructure and mechanical properties (formability and damage behaviour) under various loading and strain rate conditions is considered essential for composite materials and their applications. Certain information about the microstructure of composite materials that is difficult to anticipate through experimental tests might be predicted using finite element analysis. The influence of microstructure (size of particle and spacing between SiC particles) on the formability and damage behaviour of Al6092/17.5% SiCp composites under tensile and shear stresses at different strain rates (i.e., $1x10^{-4}$, $2x10^{-4}$, and $4x10^{-4}$ s^{-1}) was investigated in this study. A MATLAB code was developed to describe the microstructure of composite materials with varying particle sizes and spacing between particles. To evaluate the formability and damage of Al/SiC particle composites, a user-defined field (USDFLD) was developed and implemented in Abaqus/Standard based on the maximum principal stress criterion and the Rice-Tracey damage indicator. The following is a summary of the findings:

1. The distribution of SiC particles in the Al matrix influences the characteristics of Al/SiC particle composites, and superior characteristics may be obtained with uniform distribution. Under tensile and shearing loading, a large distance between particles improves formability and damage behaviour of Al/SiC particle composite.

2. The particle size has a significant impact on the formability and damage behaviour of Al/SiC particle composites; fracture in composite materials occurs around large particles. As a result, uniform and small SiC particle sizes are recommended.
3. The fracture initiation toughness of fine SiC particles is higher than that of coarse SiC particles.
4. When the spacing between SiC particles is reduced, there are more vacancies in the Al matrix, and SIC particles are concentrated in some regions, resulting in weak regions between particles that contribute to lower formability and accelerate damage initiation under tensile and shear loading.
5. The pure tensile condition is more sensitive to strain rate and particle distance than shear loading.
6. Under tensile and shear loading, the strength of the Al/SiC particle composite rises while fracture strain reduces as the strain rate increases, with the greatest strength achieved at $4\times10^{-4}S^{-1}$.
7. The designed microstructure of Al/SiC particle composite could be used to accurately predict the formability and damage behaviour of the Al/SiC particle composite materials.
8. The interface bonding between the Al matrix and the SiC particles was assumed to be perfect. Further research will be carried out to investigate matrix and interface failure under various conditions.

Acknowledgements

The authors would like to thank the Nanoscale and Microscale Research Centre (nmRC) at the University of Nottingham for access to instrumentation, as well as Dr. Christopher Parmenter, Dr. Nigel Neate, and Mr. Martin Roe, for technical assistance.

Declarations

Funding: The authors disclose that no funding, grants, or other forms of assistance were received during the preparation of this manuscript.

Conflicts of interest/Competing interests: The authors declare no competing interests.

Availability of data and material: The data included in this study are available upon request by contact with the corresponding author.

Code availability (Not applicable)

Ethics approval (Not applicable)

Consent to participate (I am agreeing to participate)

Consent for publication (I am agreeing to publish this work)

Authors' contributions: Shakir Gatea designed the study, carried out the tests, and wrote the manuscript. Tahseen Jwad developed the MATLAB code and helped evaluate the data. Fei Chen reviewed and edited the manuscript. Hengan Ou funding acquisition, designed the study, review of manuscript and contributed to the data interpretation)

References

1. Gatea, S., H. Ou, and G. McCartney, *Deformation and fracture characteristics of Al6092/SiC/17.5 p metal matrix composite sheets due to heat treatments.* Materials Characterization, 2018. **142**: p. 365-376.
2. Chen, C., S. Qin, S. Li, and J. Wen, *Finite element analysis about effects of particle morphology on mechanical response of composites.* Materials Science and Engineering: A, 2000. **278**(1-2): p. 96-105.
3. Huang, H. and M. Bush, *Finite element analysis of mechanical properties in discontinuously reinforced metal matrix composites with ultrafine micro structure.* Materials Science and Engineering: A, 1997. **232**(1-2): p. 63-72.
4. Pandorf, R. and C. Broeckmann, *Numerical simulation of matrix damage in aluminium based metal matrix composites.* Computational materials science, 1998. **13**(1-3): p. 103-107.
5. Schmauder, S., U. Weber, and E. Soppa. *Computational mechanics of heterogeneous materials: influence of residual stresses*. in *IUTAM Symposium on Computational Mechanics of Solid Materials at Large Strains*. 2003. Springer.
6. Soppa, E., S. Schmauder, G. Fischer, J. Brollo, and U. Weber, *Deformation and damage in Al/Al2O3.* Computational Materials Science, 2003. **28**(3-4): p. 574-586.
7. Mishnaevsky Jr, L., K. Derrien, and D. Baptiste, *Effect of microstructure of particle reinforced composites on the damage evolution: probabilistic and numerical analysis.* Composites Science and Technology, 2004. **64**(12): p. 1805-1818.
8. Ganesh, V. and N. Chawla, *Effect of particle orientation anisotropy on the tensile behavior of metal matrix composites: experiments and microstructure-based simulation.* Materials Science and Engineering: A, 2005. **391**(1-2): p. 342-353.
9. Tursun, G., U. Weber, E. Soppa, and S. Schmauder, *The influence of transition phases on the damage behaviour of an Al/10vol.% SiC composite.* Computational materials science, 2006. **37**(1-2): p. 119-133.
10. Mishnaevsky Jr, L.L., *Functionally gradient metal matrix composites: numerical analysis of the microstructure–strength relationships.* Composites science and technology, 2006. **66**(11-12): p. 1873-1887.
11. Zhang, W., L. Li, and T. Wang, *Interphase effect on the strengthening behavior of particle-reinforced metal matrix composites.* Computational Materials Science, 2007. **41**(2): p. 145-155.

12. Song, M. and D. Xiao, *Modeling the fracture toughness and tensile ductility of SiCp/Al metal matrix composites.* Materials Science and Engineering: A, 2008. **474**(1-2): p. 371-375.
13. Peng, Z. and L. Fuguo, *Microstructure-based simulation of plastic deformation behavior of SiC particle reinforced Al matrix composites.* Chinese Journal of Aeronautics, 2009. **22**(6): p. 663-669.
14. Ekici, R., M.K. Apalak, M. Yıldırım, and F. Nair, *Effects of random particle dispersion and size on the indentation behavior of SiC particle reinforced metal matrix composites.* Materials & Design, 2010. **31**(6): p. 2818-2833.
15. Sozhamannan, G., S.B. Prabu, and R. Paskaramoorthy, *Failures analysis of particle reinforced metal matrix composites by microstructure based models.* Materials & Design, 2010. **31**(8): p. 3785-3790.
16. Yuan, M., Y. Yang, C. Li, P. Heng, and L. Li, *Numerical analysis of the stress–strain distributions in the particle reinforced metal matrix composite SiC/6064Al.* Materials & Design, 2012. **38**: p. 1-6.
17. Tang, T., M. Horstemeyer, and P. Wang, *Micromechanical analysis of thermoelastoplastic behavior of metal matrix composites.* International Journal of Engineering Science, 2012. **51**: p. 161-167.
18. Qing, H., *Automatic generation of 2D micromechanical finite element model of silicon–carbide/aluminum metal matrix composites: Effects of the boundary conditions.* Materials & Design, 2013. **44**: p. 446-453.
19. Qing, H., *2D micromechanical analysis of SiC/Al metal matrix composites under tensile, shear and combined tensile/shear loads.* Materials & Design, 2013. **51**: p. 438-447.
20. Kukshal, V., S. Gangwar, and A. Patnaik, *Experimental and finite element analysis of mechanical and fracture behavior of SiC particulate filled A356 alloy composites: Part I.* Proceedings of the Institution of Mechanical Engineers, Part L: Journal of Materials: Design and Applications, 2015. **229**(2): p. 91-105.
21. Rangaraj, S. and K. Kokini, *Influence of particle shape and aspect ratio on thermally activated viscoplastic (time-dependent) response of ceramic (zirconia)–metal (NiCoCrAlY) particulate composites.* Materials Science and Engineering: A, 2004. **366**(2): p. 356-366.
22. Qian, L., T. Kobayashi, H. Toda, and Z.-g. Wang, *Dynamic fracture toughness of 6061Al composites reinforced with SiC particulates.* Materials Science and Engineering: A, 2001. **318**(1-2): p. 189-196.
23. Cavaliere, P., E. Cerri, and P. Leo, *Hot deformation and processing maps of a particulate reinforced 2618/Al2O3/20p metal matrix composite.* Composites science and technology, 2004. **64**(9): p. 1287-1291.
24. Ganesan, G., K. Raghukandan, R. Karthikeyan, and B. Pai, *Development of processing maps for 6061 Al/15% SiCp composite material.* Materials Science and Engineering: A, 2004. **369**(1-2): p. 230-235.
25. Davis, J., *Aluminum and Aluminum Alloys, ASM International.* Handbook Committee, 1994.
26. Lu, C., R. Danzer, and F.D. Fischer, *Fracture statistics of brittle materials: Weibull or normal distribution.* Physical Review E, 2002. **65**(6): p. 067102.
27. Needleman, A., S.R. Nutt, S. Suresh, and V. Tvergaard, *Matrix, reinforcement, and interfacial failure.* Fundamentals of metal-matrix composites(A 95-25875 06-24), Stoneham, MA, Butterworth-Heinemann, 1993, 1993: p. 233-250.
28. Rice, J.R. and D.M. Tracey, *On the ductile enlargement of voids in triaxial stress fields∗.* Journal of the Mechanics and Physics of Solids, 1969. **17**(3): p. 201-217.

29. Mishnaevsky Jr, L.L., *Computational mesomechanics of composites: Numerical analysis of the effect of microstructures of composites of strength and damage resistance*. 2007: John Wiley & Sons.